AFM study of polymer brush grafted to deformable surfaces: Quantitative properties of the brush and substrate mechanics

M. Dokukin[1], Hidenori Kuroki[2], S. Minko[3,], I. Sokolov[1,4,5,*]*

[1] Department of Mechanical Engineering, Tufts University, Medford, MA02155, USA

[2] Kanagawa Academy of Science and Technology, Kawasaki, Kanagawa 213-0012, JAPAN

[3] Nanostructured Materials Lab, University of Georgia, Athens, Georgia 30602, USA

[4] Department of Biomedical Engineering, Tufts University, Medford, MA 02155, USA

[5] Department of Physics, Tufts University, Medford, MA02155, USA

Corresponding authors: igor.sokolov@tufts.edu; s.minko@ug.edu

Polymers brushes (polymer chains end-tethered to a substrate) have been extensively studied with atomic force microscopy (AFM). Force-indentation curves are collected while squeezing the sample surface with the AFM probe. The analysis of these curves allows obtaining the equilibrium brush thickness and grafting density by using an appropriate model for mechanical deformation of the brush. However, this approach becomes inaccurate when the substrate is deformable, which is frequently the case. In this situation, the collected force-distance curves include both information about the brush and substrate deformations. Here we describe a method which takes into account both the brush and substrate deformations. Quantitative accuracy of the presented method is demonstrated by applying the method to measuring a polyethylene oxide brush grafted to the cross-linked poly (2-vinyl pyridine) substrate swollen in aqueous media of different acidity. By analyzing the AFM force curves, we simultaneously obtain the grafting density, equilibrium brush thickness, and the Young's modulus of the substrate. The method is verified by independent measurements of the substrate Young's modulus and direct measurements of the brush thickness using ellipsometry. The method demonstrates a very good agreement between the estimated and directly measured Young's modulus of the substrate and molecular characteristics of the brush.

Introduction

Polymer chains end-tethered to a substrate (*aka* polymer brushes) are of great interest for building complex functional interfaces. Such interfacial structures demonstrate feasibility to control and regulate interactions between particulates and planar surfaces of materials. It is broadly used in living systems and synthetic materials[1-3]. A kind of polymer brush architectures are found in biological organisms, for example, on cell membrane that is decorated with biopolymer brushes [4-7] or in bone cartilage [8-10]. Colloidal stabilization [11-12], antifouling coatings[13-15], invisible for immune system hydrogel coatings of capsules for targeted drug delivery[16-17] and various biointerfaces[18] are a few examples when brush architecture is routinely used for industrial and biomedical applications.

Polymer brush is characterized by molecular mass of the grafted chains, grafting density and polymer –solvent interaction. A combination of these characteristics results in the equilibrium thickness of the brush owing to the osmotic pressure leveraged by entropy loses of the stretched polymer coils of the brush [19-20]. Experimentally, the brush characteristics can be extracted from measurements of the brush thickness, polymer density profiles and molecular mass of grafted chains. For the case of a dry sample of the brush, measurement of the brush thickness can be done, for example, by means of ellipsometry or X-ray reflectivity. Such measurements provide sufficient information to estimate the grafting density (provided known molecular mass of the polymer). For the brushes synthesized by grafting polymers from the surface of the substrate, characterization of the brush is limited due to challenges of characterization of the molecular mass of the grafted polymer. A common approach is to measure molecular mass of the bulk polymer synthesized in the solution above the solid substrate, and assume that the mechanism of the chain formation is the same on the surface and in the bulk. The polymer molecular mass and grafting density can be used then to predict polymer brush interaction with solvent, particulates and solid surfaces. However, in many cases the amount of polymer formed in the solution above the solid substrate is negligible so that the grafted brushes cannot be characterized properly. Thus, it is important to find experimental methods for characterization of polymer brushes for samples in which the molecular mass of the grafted chains cannot be measured directly.

Atomic force microscopy (AFM) [21] is one of comprehensive methods to study polymer brush characteristics via the analysis of AFM tip-polymer brush interactions. The latter information can be derived from force-indentation curves that AFM can record in each point of the sample surface. The data can be collected when AFM operates in HarmoniX, PeakForce QNM AFM modes (from Bruker-Nano, and similar modes from other AFM manufacturers) [22-24], and a classical force-volume mode [25-26]. The force-volume mode, being rather slow compared to others, allows a better control over the scanning parameters. Importantly, the force-volume mode can be operated at relatively slow vertical (ramping) speed. This decreases possible hydrodynamic drag artifacts when studying soft surfaces, and in particular, polymer brushes. Essentially the AFM technique gives a direct experimental evaluation of mechanical response of polymer brushes grafted to different substrates.

Although, AFM was used to extract the parameters of the polymer brush, see, e.g., [26], the brush was attached to a relatively rigid substrate. In many cases, polymer brushes are attached to relatively soft (deformable) polymer substrates. While compressing (indenting) deformable samples covered with a polymer brush, the AFM probe simultaneously deforms both the brush and the soft substrate. A model that takes into account deformations of both brush and substrate simultaneously has been initially developed to characterize mechanical response, for example, of biological cells [4, 27-29]. The model allows to separate the mechanical deformation of the cell body from the deformation of the brush-like structure formed by the molecules at the extracellular (brush) layer. However, it is difficult to verify that model quantitatively due to a high complexity of the substrate (cell body).

The goal of this work is to verify the proposed mechanical model of the polymer brush grafted to a deformable substrate using well-characterized synthetic sample, and therefore, to demonstrate that the AFM technique is capable of quantitative measurements of the brush parameters as well as the mechanics of the deformable substrate. The synthetic material used here is polyethylene oxide (PEO) brush grafted to the surface of a cross-linked poly (2-vinyl pyridine) (P2VPxl) substrate. Swelling of P2VPxl in water depends on pH, while the effect of pH on the mechanical response of PEO brushes is negligible. Thus, mechanical properties of P2VPxl substrate can be tuned via changes in pH so that the cumulative response of the PEO brush on P2VPxl substrate is modulated by the response of the substrate with no substantial

changes in the PEO brush characteristics. In addition, the mechanics of the P2VPxl substrate is independently measured before grafting the brush. Finally, the brush parameters are independently measured by the ellipsometry technique. We see a very good agreement between the estimated and directly measured Young's modulus of the substrate and molecular characteristics of the brush..

EXPERIMENTAL DETAILS

Materials

Poly(2-vinyl pyridine) (P2VP, M_n = 152 Kg/mol), diiodobutane (DIB), 4-propylphenol, and 5-bromovaleryl chloride (Sigma-Aldrich); 11-bromoundecyldimethylchlorosilane (Gelest, inc.); poly(ethylene oxide) methylether with the end functional hydroxyl group (PEO-OH, M_n = 12.3 Kg/mol, polydispersity index 1.1, Polymer Source) were used as received. Bromo-terminated poly(ethylene oxide) (PEO-Br) was synthesized via the reaction of PEO-OH with 5-bromovaleryl chloride according to the procedure reported in the literatures [30].

Synthesis of PEO-brushes on P2VPxl film

The cross-linked P2VP films on the surface of Si-wafers (shown in figure 1) were prepared according to the following procedure: [30-32] 2 w/v% P2VP and 2 vol% DIB were dissolved in a mixture of nitromethane and tetrahydrofuran (volume ratio of 9:1). The resulting solution was heated at 80°C with stirring for different periods of time to approach a desired degree of quaternization. In this stage, P2VP is functionalized with DIB when majority of DIB is reacted by one functional group resulting in the functional P2VP with iodobutane side functional groups. It is noteworthy, that the heating time of the P2VP –DIB mixture in solution is controlled to reach a quarternization degree greater than 5%. In our previous study[30], it was found that if the quaternization degree was less than 5%, PEO with molecular weight of 12.3 Kg/mol penetrated inside the crosslinked P2VP network. In contrast, PEO did not penetrate a highly-crosslinked P2VP film, at a greater than 5% quaternization degree, and thus PEO can be grafted only on the surface of P2VPxlfilm. Afterward, the solution was filtered, and diluted to half with the same mixture solvent of nitromethane and tetrahydrofuran. Prior to spin-coating, 0.25 vol% of 4-

propylphenol was added into the solution to prevent the phase separation of quaternized P2VP and DIB. The obtained solution was spin-coated on the surface of silanized silicon wafers at 3000 rpm at a low ambient humidity (< 10 RH%). The silanization of the silicon wafers was carried out by immersing them in 1 wt% 11-bromoundecyldimethylchlorosilane solution in dry toluene at room temperature overnight. The resulting films were annealed at 100ºC in vacuum for at least 1h to complete the cross-linking reaction of P2VP with residual functional groups of DIB, and the immobilization reaction of the P2VPxl film via bromoalkyl groups on the silicon wafers. The prepared P2VPxl films were characterized by using FTIR spectroscopy. The quaternization degrees of 6.4% was obtained for the heating times of P2VP-DIB mixtures for 1h. Thus, the reaction time for quaternization was set at 1h for all sample preparations to ensure the formation of only surface grafted PEO brushes on P2PVxl films.

Afterward, PEO was grafted to the surface of the P2VPxl films. A 2 w/v% solution of bromo-terminated PEO in toluene was spin-coated on the P2VP network films at 3000 rpm, and then the grafting reaction was conducted by annealing at 120°C in vacuum for 20h. After the grafting step, the films were rinsed with chloroform and an acidic aqueous solution (pH 2.0) for 1 day for each solvent to remove unreacted PEO, and then dried with a N_2 gas flow.

PEO brush on P2VPxl film characterization

To measure the dry film thickness (and consequently, to estimate the grafting density), PEO-grafted P2VP samples were characterized using ellipsometry. The Multiskop null-ellipsometer (Optrel) equipped with a He-Ne laser (λ = 633 nm) was used for ellipsometric measurements. The angle of incidence of polarized light was set to 70°.

The AFM scratch test [33] was also performed to estimate film thickness in air and in water (at pH 5.5). In the scratch test, a sharp steel needle was used to scratch the film down to the surface of the silicon substrate, producing a step with a height equal to the film thickness. Note that the AFM tip does not damage the harder Si wafer surface. The absence of Si wafer damage after the scratch was verified during AFM imaging. The AFM imaging in air and in water was conducted using Dimension 3100 and MultiMode scanning probe microscopes (Bruker Nano/Veeco, Inc) operating in the standard tapping mode. NPS silicon nitride probes (Bruker Nano, CA, USA)

with a spring constant of 0.32 N/m (estimated as described in[34]), a resonance frequency in aqueous media of ~9 kHz, and the radius of the tip curvature of 20 nm (nominal) were used for scanning.

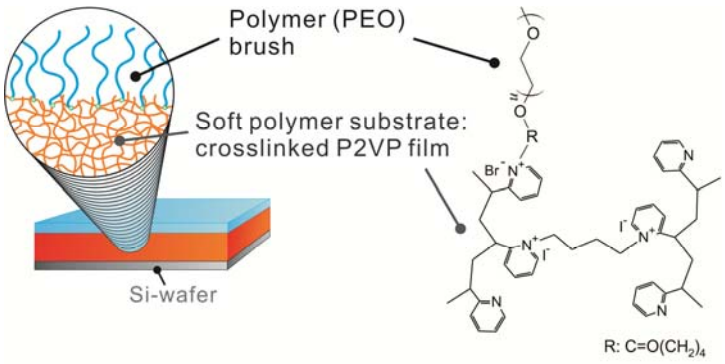

Figure 1. Schematic illustration of PEO-grafted P2VP flat thin film. Polymer brush is grafted on a deformable polymer substrate.

AFM force-volume imaging

Dimension 3100 (Veeco, Inc.) AFM with Nanoscope V controller and NPoint close-loop scanner (200 μm × 200 μm × 30 μm, XYZ) were used for all force measurements in this study. The annealed SHOCON (AppNano, Santa Clara, CA) probe with radius of R=105±10 nm and spring constant of 0.29±0.04 N/m was utilized. The spring constant was calibrated using thermal tune method [35-36]. Standard cantilever holder for operation in liquids was used. Force-indentation curves were recorded with vertical speed of 1 μm/s (1 Hz ramp rate and 500nm Z ramp size). For each sample, the force volume maps with size of 10x10 μm^2 and resolution of 16x16 pixels were collected from several different regions. When operating in the force-volume mode, the AFM probe approaches the brush-coated surface and deforms the brush. The force-separation curves are recorded for each point. The acidity of the aqueous medium (1mM of NaCl) was adjusted with the help of HCl.

Mechanical model of deformation of polymer brush on a deformable substrate

The brush on a deformable substrate model is the method to find the force response due to deformation of an elastic homogeneous material covered with a second material that has a negligible lateral stress (close to zero Poisson ratio) [4, 37]. In the particular case of this work, the second material is a polymer brush. Furthermore, in contrast to the previous works, both polymer brush and substrate are well-defined and characterized materials. Below is a brief description of the model.

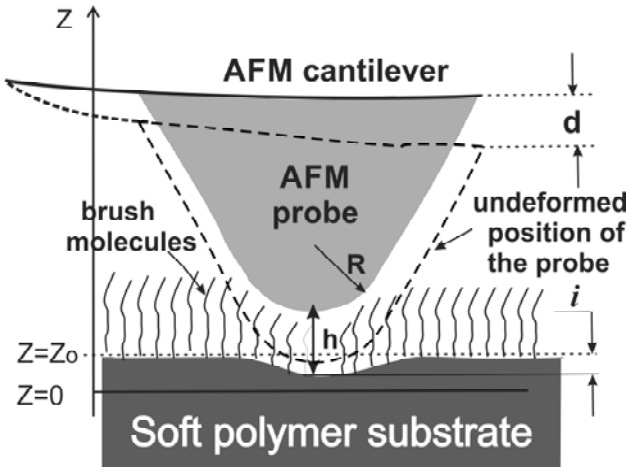

Figure 2. A schematic of an AFM probe over a deformable deformable surface covered with a grafted polymer brush. Z is the relative position of the cantilever, d is the cantilever deflection, Z_0 non deformed position of the substrate surface, i deformation of the substrate and h is the separation between the substrate surface and the AFM probe. Z is set to 0 for the maximum cantilever deflection.

Figure 2 shows a schematic of an AFM probe interacting with a typical deformable surface covered with a polymer brush. Mechanical deformation of the substrate and long-range force (due to steric repulsion) cause the deflection of the cantilever *d*. The load force *F* is described by the Hooke's law, $F=kd$, where *k* is the spring constant of the AFM cantilever. *Z* is the vertical position of the cantilever shown in figure 2. It is assumed that Z=0 for the maximum cantilever deflection d_{max}. $Z=Z_0$ is non-deformed position of the deformable substrate and *d* is the substrate deformation. *h* is the separation between the substrate surface and the AFM probe. From the

diagram shown in figure 2, one can see the following relationship between all presented parameters:

$$h = Z - Z_0 + \left[\frac{3\left(1-\nu^2\right)}{4} \frac{kd}{E} \sqrt{\frac{R_t + R_s}{R_t R_s}} \right]^{2/3} + d\,, \tag{1}$$

where R_s is the radius of curvature of the substrate at the point of contact, R_t is the radius of the probe and ν is the substrate Poisson ratio, E is the elastic modulus of the substrate.

Because Z is defined as zero when $d=d_{max}$, we can exclude Z_0 from the equation (1):

$$Z = \left[\frac{3\left(1-\nu^2\right)}{4} \frac{k}{E} \sqrt{\frac{R_t + R_s}{R_t R_s}} \right]^{2/3} (d_{\max}{}^{2/3} - d^{2/3}) + (d_{\max} - d) + h\,. \tag{2}$$

As shown previously [4, 38], the unknown parameters E and h can be found by using the following procedure. Assuming that the force imposed by the cantilever close to its maximum deflection (kd_{max}) is sufficient to completely "squeeze" the molecular brush between the AFM probe and the substrate surface one can set the $h=0$ near that maximum force. This assumption relies on a much smaller stiffness of the molecular brush layer compared to the stiffness of the substrate polymer, but it certainly depends on the value of d_{max}. It has to be sufficiently large to ensure enough load force to completely squeeze the molecular brush. This can be verified post-factum, after the parameters of the brush being derived, and should be kept in mind when doing measurements. When the molecular brush is squeezed to a higher degree, the brush behavior can turn into the behavior of an elastic material. Furthermore, it is obvious that the effective stiffness of the brush is increasing with the brush compression. At one point, the stiffness of the substrate will be equal to the stiffness of the squeezed molecular brush, and therefore, their elastic responses will become similar. Thus, the error due to the deviation h from zero can be assigned to the uncertainty in the indentation depth. For example, if we consider 90% deformation of the brush as a good approximation of completely squeezed brush layer, the error of 10% would result in maximum error of 1 nm for a maximum indentation depth of 10 nm. This is quite acceptable for the present degree of quantitative analysis (~ 15% error in definition of the elastic modulus E). The approach described above allows to unambiguously derive the force related to

the polymer brush layer as well as the Young's modulus of the substrate. Assuming *h=0* around the point of maximum load, equation (2) can be written as:

$$E = \frac{3\left(1-\nu^2\right)}{4} k \sqrt{\frac{R_t + R_s}{R_t R_s}} \left(\frac{d_{\max}^{2/3} - d^{2/3}}{Z - d_{\max} + d} \right)^{3/2} \approx$$
$$\approx \frac{\left(1-\nu^2\right)}{2} \sqrt{\frac{2}{3}} k d_{\max}^{-1/2} \sqrt{\frac{R_t + R_s}{R_t R_s}} \left(\frac{d_{\max} - d}{Z - d_{\max} + d} \right)^{3/2} \Bigg|_{d \to d_{\max}} \quad (3)$$

The repulsion force due to the brush layer $F_{brush}(h)$ can now be found by using the following inexplicit equations:

$$F_{brush}(h) = kd, \quad h(d) = Z - \left[\frac{3\left(1-\nu^2\right)}{4} \frac{k}{E} \sqrt{\frac{R_t + R_s}{R_t R_s}} \right]^{2/3} \left({d_{\max}}^{2/3} - d^{2/3} \right) - \left(d_{\max} - d \right). \quad (4)$$

To calculate the brush parameters, the equilibrium brush size *L* and grafting density *N*, using $F_{brush}(h)$ data, one needs to use a model describing the force due to the polymer brush. Following the approach used in the literature, we model this force using the following equation [4, 27-28, 38-39]:

$$F_{brush} = F_{steric} \approx 100 k_B T \sqrt{\frac{R_t R_s}{R_t + R_s}} N^{3/2} \exp\left(\frac{-2\pi h}{L} \right) L, \quad (5)$$

where *h* is the probe-surface distance, *R* is the radius of the AFM probe, and *T* is the medium temperature. Note the difference by the factor of two compared to the original citations; this is done to correct the error propagated from the original work [39]. Equation (5) can be used for the numerical fitting of experimental data. This equation is a good approximation for a limited interval of *h*: $0.2<h/L<0.9$.

It should be noted that further development of equation (5) within the Derjaguin approximation has been recently reported in [40], when the effect of sharpness of the AFM probe was studied for the brushes immersed in different solvents. The analysis of those modified equations is beyond the scope of this work, the use of the present model is justified by a good quantitative agreement obtained by means of equation (5).

Results and Discussion

Two similar P2VPxl samples were synthesized and characterized to verify reproducibility of the sample preparation. The thickness of dry P2VP films, estimated by ellipsometry, was found to be 42.2±0.5nm and 42.3±0.4nm for two samples. The measurements were verified with AFM by measuring of depth of the trench scratched on the sample surfaces using a steel needle. The AFM measurements provided results for P2VPxl thicknesses for both the samples at 40.1±0.5nm. One sample was used for the mechanical measuring the Young's modulus of the P2VPxl film. The second sample was used for the grafting of a PEO brush (P2VPxl-PEO) for subsequent measurements of the parameters of the brush and the Young's modulus of the substrate, the P2VPxl film. After grafting PEO brush to P2VP film, the dry thickness of the PEO brush was found to be 6.5±0.1nm from ellipsometry measurements and 6.7±0.5nm from the AFM scratch. Amount of the grafted PEO, Γ, was calculated from the ellipsometric dry thickness, h (nm), and the density (ρ = 1.09 g/cm^3) of PEO using the equation: $\Gamma = h\rho$ (mg/m^2). The grafting density of PEO, N, was estimated by using the following equation: $N = \frac{\Gamma \cdot N_A}{M_n} \times 10^{-21}$ (nm^{-2}), where N_A (mol^{-1}) is the Avogadro number, M_n (g/mol) is the number average molecular weight of PEO [41]. Using the following parameters of the dry brush: h = 6.5 nm, Γ = 7.0 mg/m^2, M_n = 12300 g/mol, one obtains an estimated value of N=0.32 nm^{-2} .

The thickness of the swollen PEO brush in pH 5.3 buffer was estimated using the same approach of measuring of the scratched trench depth. The swollen brush thickness was obtained as the difference of the trench depth for the P2VPxl-PEO sample and the trench depth for P2VPxl sample without PEO brush. The obtained value was found to be 16.5 ± 3 nm. it is worth noting that the trenches where scanned at different load forces, from a high force to a low force to find the minimal force when the tip-brush mechanical contact was detected. This procedure provided the lowest possible compression of the brush by the AFM tip. A particular pH was chosen to avoid excessive swelling of the substrate.

To study the brush and mechanical properties of the substrate using the described method, an AFM probe of sufficiently large diameter was used. Such a probe was taking to avoid

the artifacts of nonlinearity which are typically seen when using sharp commercial probes [42-43]. Mechanical properties of P2VPxl films depend on the acidity of the immersing buffer. By changing pH from 5.3 to pH 2, we change the mechanical properties of the P2VPxl substrate owing to changes of the ionization degree of pyridine monomer units. Therefore, the experiments were carried out in two different immersing buffers with pH 2.0 and 5.3.

Typical force-indentation curves (raw data as recorded by the microscope) are presented in figure 3. One can see a substantially different behavior of the force curves collected on the P2PVxl substrates with and without PEO brush. In addition, there is a clear difference in the mechanical response of the system observed in buffers with pH 2.0 and 5.3.

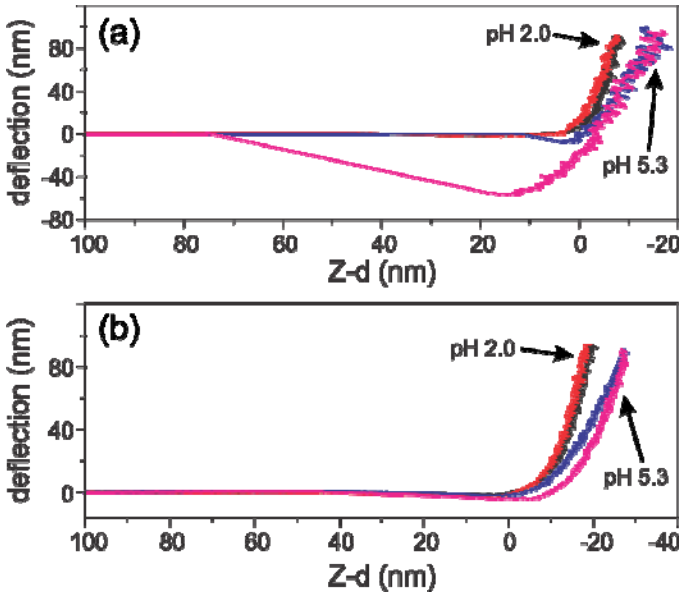

Figure 3. Typical force-indentation curves collected on (a) P2PVxl and (b) P2VPxl-PEO. The deflection of the cantilever *d* on the separation distance (*Z-d*) is shown (Z is the vertical position of the AFM scanner).

Analysis of the data exampled in figure 3 is presented in figure 4. The approaching part of force curves were analyzed to avoid any artifacts related to the slow relaxation or potential damage of the brush layer. The data points near the maximum load force are fitted with equation 2 (the Hertz model, deformation of the elastic substrate with no brush), and consequently, extrapolated to lower forces. One can see that sample P2VPxl (figure 4(a)) shows almost ideal fit

of the Hertz model, whereas sample P2VPxl-PEO (figure 4(b)) can be described well with the Hertz model only for the large force, thick solid (green online) top part of the curve. The thin solid (red online) part of the curve is the extrapolation for smaller forces. One can see a substantial deviation from the behavior of an elastic material, from the Hertz model. This agrees well with our brush-on-the deformable-substrate-model described by equations 1-4. The fit with the Hertz model gives the value of the Young's modulus, which can be found using equation 3. As a next step, the force due to the brush is derived from the experimental data using equation 4. This force is exampled in figure 4c. The force data are presented in the logarithmic scale. One can clearly see the exponential behavior (a straight line in the logarithmic scale). This data are fitted with equation 5 to extract the brush parameters, the equilibrium length L and grafting density N.

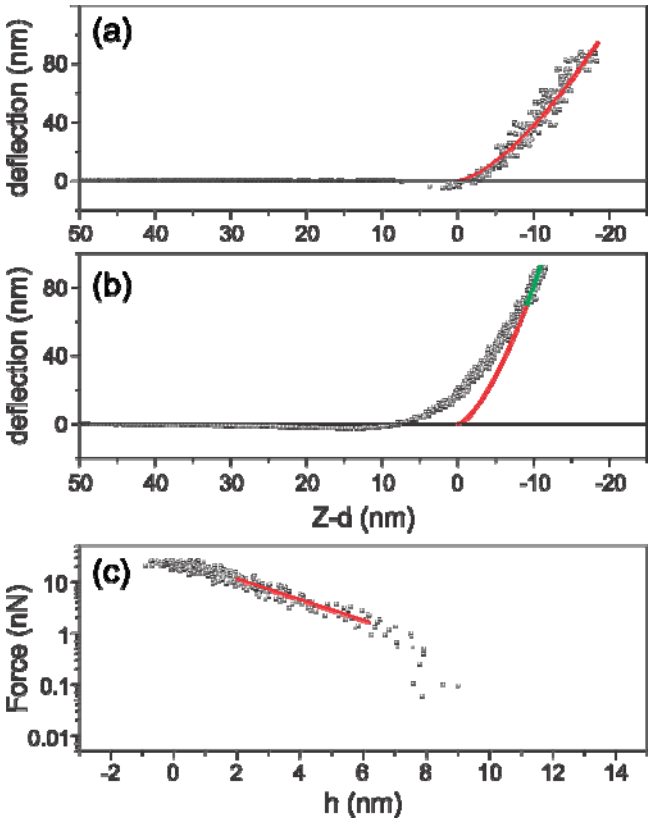

Figure 4. An example of processing experimental force-indentation data with the Hertz part of the model (equation (2)). (a) The fitting of the bare P2VPxl polymer sample and

(b) the same sample covered with the PEO polymer brush (P2VPxl-PEO). The force due to PEO brush (c) derived using equation (4) from the data shown in panel (b).

It is important to note the presence of the AFM probe-surface adhesion in the case of P2VPxl sample with no brush for pH5.3, Figure 3a. The presence of such interaction is taken into account by the use of appropriate contact model which takes into account adhesion, for example, JKR or DMT models [43]. The choice between the JKR and DMT models can be done based on the use of the Maugis parameter α [44-45], which is a dimensionless parameter ranging between 0 and 1. α close to 1 justifies the use of the JKR model, whereas α close to 0 points to the use of the DMT model. The Maugis parameter α can be found using the following formula [44]: $\alpha = -50/51\left(\exp[-250\lambda/231]-1\right)$, where $\lambda = 1.1570/D_0^3 * \left(w_{adh}^2 R / E^{*2}\right)^{1/3}$ [44-45], w_{adh} is the adhesive energy per unit area, R is the probe radius, $E^* = E/\left(1-\nu^2\right)$ is the "reduced" Young's modulus, and ν is the Poisson ratio. D_0 is the interatomic distance between the atoms of probe and sample at contact. The adhesive energy per unit area can be found from the adhesion force [43]. For example, the surface energy in the case of pH5.3 can be found as 0.036±0.005 J/m^2. D_0 is taking assuming the adhesion originates at the van der Waals interaction; it typically ranges within 0.15-0.17 nm [19, 43, 46]. Using these values, one can find that Maugis parameter α~0.98, which means the choice of JKR model.

The absence of nonlinearity and influence of the substrate is verified by one of the most comprehensive tests, testing the obtained elastic moduli as the function of the indentation depth. The linearity of the stress-strain response manifests itself in independence of elastic modulus of the indentation depth. Figure 5 shows typical behavior of the modulus on the different indentation depth. One can see virtually no dependence. Thus, one can conclude that we work in the linear stress-strain regime.

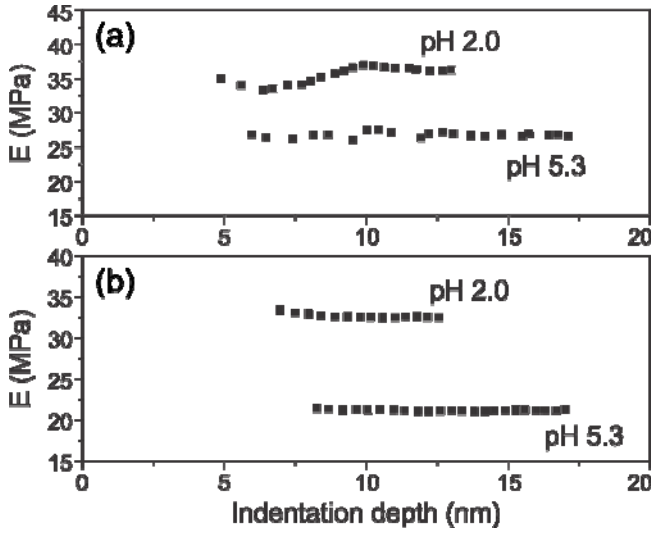

Figure 5. Typical dependence of the elastic modulus on the indentation depth for (a) P2VPxl and (b) P2VPxl-PEO samples are shown for two different pH (2.0 and 5.3).

The model described above was applied to 40 force curves collected for each sample at pH 2.0 and 5.3 (160 force curves in total). Statistical histograms of the obtained results are shown in Figures 6 and 7. Figure 6 shows histograms of the obtained distributions of the Young's modulus of the P2VPxl film with and without the grafted PEO brush. As was mentioned, mechanical property of P2VPxl depends on the acidity of the environment. Figure 6 presents the results of measurements for P2VPxl immersed in buffers with two different pH, 2.0 and 5.3. One can see that the average values of the Young's modulus are indeed changing with change of pH. The mean values demonstrate virtually identical for both samples ~2.1x increase of the Young's modulus with the decrease of pH. From this observation, one can make an interesting conclusion that the overall elastic response of P2VPxl film is presumably defined by a strong electrostatic repulsion. This repulsion is stronger for lower pH, and consequently, can result in higher elastic modulus.

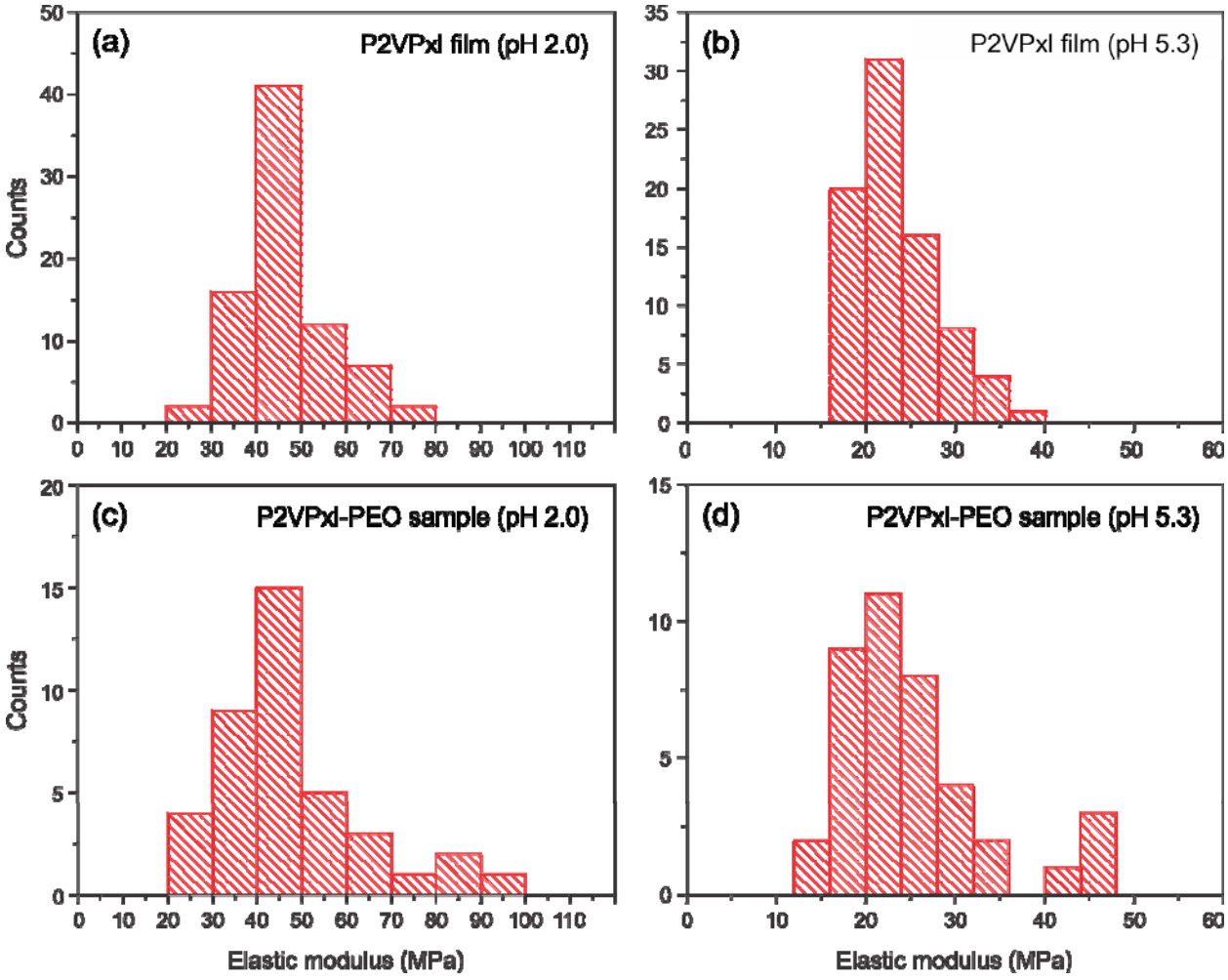

Figure 6. Histograms of the elastic (Young's) modulus of P2VPxl film (a, b)) and P2VPxl-PEO sample (c, d)) measured at two different pH.

Comparing the values of the Young's modulus obtained for P2VPxl films with and without PEO brush, one can see that the brush model rather accurately defines the Young's modulus of the P2VPxl for both pH. The average modulus of P2VPxl film in pH 5.2 with brush is (25±8.4)MPa and (23±4.3)MPa without brush. The average modulus of P2VPxl film in pH 2.0 with brush is (48±15)MPa and (46±9.5)MPa without brush. This verifies the part of the brush model that defines the mechanical properties of the polymer substrate layer.

Figure 7 shows histograms of the distributions of the brush parameters calculated for P2VPxl-PEO sample measured in two different buffers with pH 2.0 and 5.3. It is worth noting that the obtained force dependence due to the brush can be analyzed by different models [39-40, 47]. Here we choose the model described by equation (5) as a nonrestrictive example. The values of the grafting density estimated using this model N=0.57±0.04 nm^{-2} for pH 2.0 and N=0.55±0.09 nm^{-2} for pH 5.3. These values are statistically the same for both pH, thus indicating the expected no effect of the state of the deformable substrate on the molecular characteristics of the brush. This is expected because PEO molecules in the brush are very weekly charged, and as a result, the size of the brush is not pH dependent [48]. However, both values are greater than the values derived from the direct measurements of dry brush thickness, N=0.32 nm^{-2}. This discrepancy might be explained by the deficiency of the model that does not take into account specific solvent-brush interactions and a partial blending of PEO and P2VP at the grafting interface.

As to the length of the brush derived from the mechanical probing, we also observed the expected virtually no change of the length of the brush with changing pH, L=19±1.7nm at pH 2.0 and L=16±1.7nm at pH 5.3. It is worth noting that the observed slight increase of the brush length is in agreement with the hypothesis about partial blending of PEO and P2VP at the grafting interface. P2VP molecules are higher protonated in lower pH, and as a result, may be stretched more at pH2 compared to pH5.3. When comparing these brush lengths with the value obtained from the direct measurements (~16 nm), one can see a very good match.

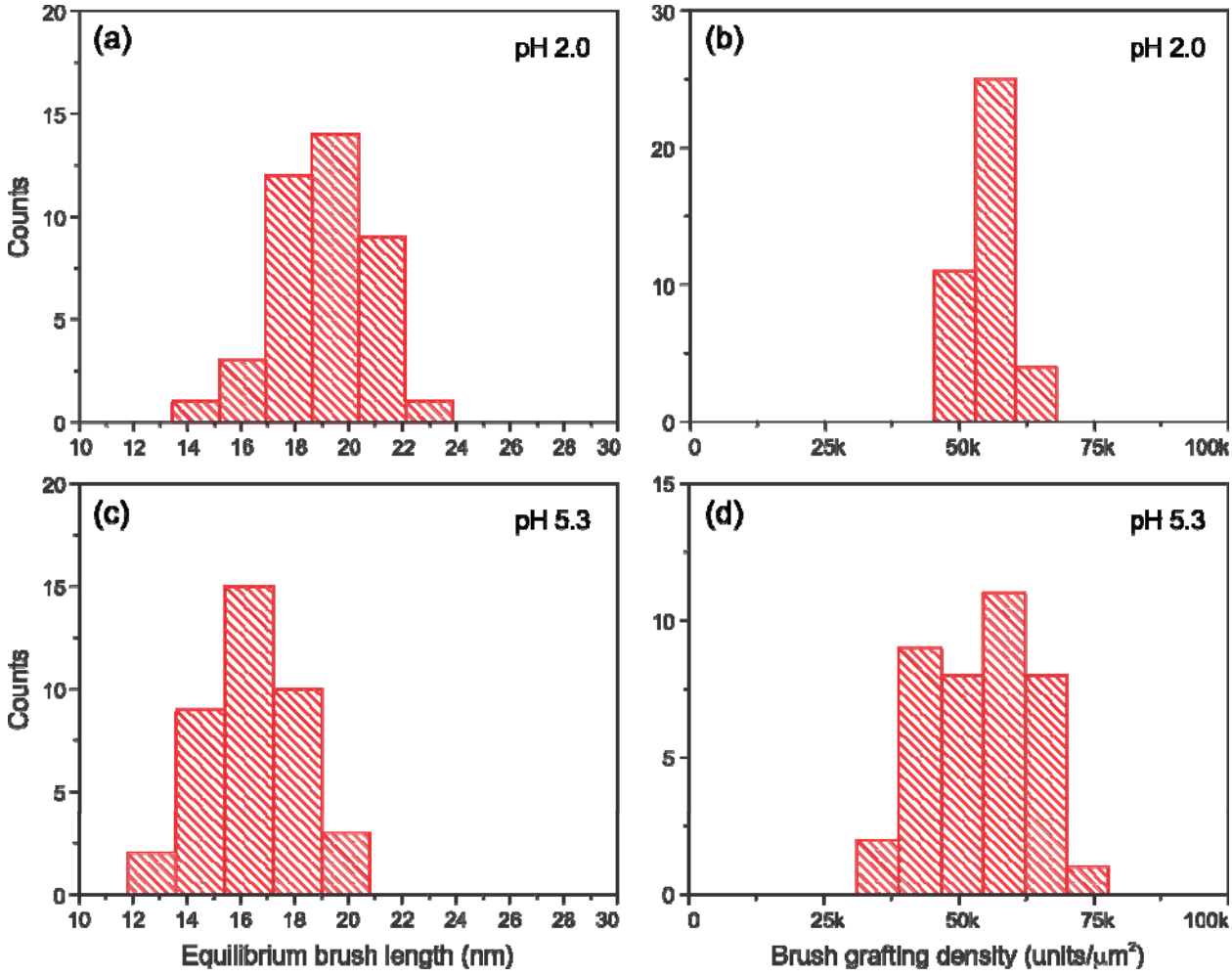

Figure 7. Histograms of the PEO brush length *L* (a, c) and grafting density *N* (b, d) distributions derived for *P2VPxl-PEO* at two different pH.

Conclusion

We demonstrated a very good quantitative nature of the model we suggest to use to analyze AFM force curves collected on a polymer brush grafted to a deformable substrate. The model allows to qualitatively separate the mechanical response of the polymer substrate and brush layer. The results demonstrate very good agreement between the values of the Young's modulus of the polymer substrate measured directly (without brush) and derived using the model described here from the measurements on the polymer covered with brush. Furthermore, the

equilibrium length of the brush is in excellent agreement with the one found independently. A discrepancy in the grafting density with a factor 1.5 (tolerable for many quantitative estimations) might be explained by the deficiency of the brush layer model that should be adjusted for specific polymer-solvent interactions and interpenetration of a small fraction of P2VP strands of the substrate network in the PEO brush. This calls for systematic studies of mechanical response of the brush in solvents of different quality grafted to the surface of substrates immiscible with polymer brush. Thus, we can conclude that we presented an AFM method capable of quantitative characterization of the brush grafted to deformable substrates. In addition, the mechanical properties of the underlined substrate can be simultaneously and reliably measured in a quantitative manner.

ACKNOWLEDGEMENT

Financial support from the National Science Foundation (CMMI 1435655 (I.S.) and DMR 1426193 (S.M.)) is gratefully acknowledged. Any opinions, findings, and conclusions or recommendations expressed in this material are those of the author(s) and do not necessarily reflect the views of the National Science Foundation.

REFERENCES:

1. Vargas-Pinto, R.; Gong, H.; Vahabikashi, A.; Johnson, M., The Effect of the Endothelial Cell Cortex on Atomic Force Microscopy Measurements. *Biophysical Journal* **2013,** *105* (2), 300-309.

2. Zhou, R.; Zhou, H.; Xiong, B.; He, Y.; Yeung, E. S., Pericellular matrix enhances retention and cellular uptake of nanoparticles. *J Am Chem Soc* **2012,** *134* (32), 13404-9.

3. Brittain, W. J.; Minko, S., A structural definition of polymer brushes. *J. Polym. Sci., Part A: Polym. Chem.* **2007,** *45* (16), 3505-3512.

4. Sokolov, I.; Iyer, S.; Subba-Rao, V.; Gaikwad, R. M.; Woodworth, C. D., Detection of surface brush on biological cells in vitro with atomic force microscopy. *Applied Physics Letters* **2007,** *91*, 023902-1-3.

5. Dokukin, M.; Ablaeva, Y.; Kalaparthi, V.; Seluanov, A.; Gorbunova, V.; Sokolov, I., Pericellular Brush and Mechanics of Guinea Pig Fibroblast Cells Studied with AFM. *Biophys J* **2016,** *111* (1), 236-46.

6. van Oosten, A. S.; Janmey, P. A., Extremely charged and incredibly soft: physical characterization of the pericellular matrix. *Biophys J* **2013,** *104* (5), 961-3.

7. Clarris, B. J.; Fraser, J. R., On the pericellular zone of some mammalian cells in vitro. *Experimental cell research* **1968,** *49* (1), 181-93.

8. Rojas, F. P.; Batista, M. A.; Lindburg, C. A.; Dean, D.; Grodzinsky, A. J.; Ortiz, C.; Han, L., Molecular adhesion between cartilage extracellular matrix macromolecules. *Biomacromolecules* **2014,** *15* (3), 772-80.

9. Stolz, M.; Gottardi, R.; Raiteri, R.; Miot, S.; Martin, I.; Imer, R.; Staufer, U.; Raducanu, A.; Duggelin, M.; Baschong, W.; Daniels, A. U.; Friederich, N. F.; Aszodi, A.; Aebi, U., Early detection of aging cartilage and osteoarthritis in mice and patient samples using atomic force microscopy. *Nat Nanotechnol* **2009,** *4* (3), 186-92.

10. Han, L.; Grodzinsky, A. J.; Ortiz, C., Nanomechanics of the Cartilage Extracellular Matrix. *Annu Rev Mater Res* **2011,** *41*, 133-168.

11. Saville, S. L.; Woodward, R. C.; House, M. J.; Tokarev, A.; Hammers, J.; Qi, B.; Shaw, J.; Saunders, M.; Varsani, R. R.; St Pierre, T. G.; Mefford, O. T., The effect of magnetically induced linear aggregates on proton transverse relaxation rates of aqueous suspensions of polymer coated magnetic nanoparticles. *Nanoscale* **2013,** *5* (5), 2152-63.

12. Elbert, D. L.; Hubbell, J. A., Self-assembly and steric stabilization at heterogeneous, biological surfaces using adsorbing block copolymers. *Chem Biol* **1998,** *5* (3), 177-83.

13. Pesek, S. L.; Li, X. Y.; Hammouda, B.; Hong, K. L.; Verduzco, R., Small-Angle Neutron Scattering Analysis of Bottlebrush Polymers Prepared via Grafting-Through Polymerization. *Macromolecules* **2013,** *46* (17), 6998-7005.

14. Li, X. Y.; Prukop, S. L.; Biswal, S. L.; Verduzco, R., Surface Properties of Bottlebrush Polymer Thin Films. *Macromolecules* **2012,** *45* (17), 7118-7127.

15. Kuroki, H.; Tokarev, I.; Minko, S., Responsive Surfaces for Life Science Applications. *Ann. Rev. Mater. Res.* **2012,** *42*, 343-372.

16. Yoshimoto, K.; Nishio, M.; Sugasawa, H.; Nagasaki, Y., Direct observation of adsorption-induced inactivation of antibody fragments surrounded by mixed-PEG layer on a gold surface. *Journal of the American Chemical Society* **2010,** *132* (23), 7982-9.

17. Motornov, M.; Roiter, Y.; Tokarev, I.; Minko, S., Stimuli-responsive nanoparticles, nanogels and capsules for integrated multifunctional intelligent systems. *Prog Polym Sci* **2010,** *35* (1-2), 174-211.

18. Zhou, J.; Tam, T. K.; Pita, M.; Ornatska, M.; Minko, S.; Katz, E., Bioelectrocatalytic System Coupled with Enzyme-Based Biocomputing Ensembles Performing Boolean Logic Operations: Approaching "Smart" Physiologically Controlled Biointerfaces. *ACS Appl. Mater. Interfaces* **2009,** *1* (1), 144-149.

19. Butt, H.-J. r.; Kappl, M., *Surface and interfacial forces*. Wiley-VCH: Weinheim, 2010; p xv, 421 p.

20. Israelachvili, J. N., *Intermolecular and surface forces : with applications to colloidal and biological systems*. Academic Press: London ; Orlando, Fla . 1985; p xv, 296 p.

21. Binnig, G.; Quate, C. F.; Gerber, C., Atomic force microscope. *Phys. Rev. Lett.* **1986,** *56* (9), 930-933.

22. Sahin, O.; Magonov, S.; Su, C.; Quate, C. F.; Solgaard, O., An atomic force microscope tip designed to measure time-varying nanomechanical forces. *Nature Nanotechnology* **2007,** *2*, 507 - 514.

23. Schon, P.; Bagdi, K.; Molnar, K.; Markus, P.; Pukanszky, B.; Vancso, G. J., Quantitative mapping of elastic moduli at the nanoscale in phase separated polyurethanes by AFM. *Eur. Polym. J.* **2011,** *47* (4), 692-698.

24. Sweers, K.; van der Werf, K.; Bennink, M.; Subramaniam, V., Nanomechanical properties of alpha-synuclein amyloid fibrils: a comparative study by nanoindentation, harmonic force microscopy, and Peakforce QNM. *Nanoscale Research Letters* **2011,** *6*.

25. Hoh, J. H.; Schoenenberger, C. A., Surface morphology and mechanical properties of MDCK monolayers by atomic force microscopy. *J Cell Sci* **1994,** *107 (Pt 5)*, 1105-14.

26. Volkov, D.; Strack, G.; Halamek, J.; Katz, E.; Sokolov, I., Atomic force microscopy study of immunosensor surface to scale down the size of ELISA-type sensors. *Nanotechnology* **2010,** *21* (14), 145503.

27. Guz, N.; Dokukin, M.; Kalaparthi, V.; Sokolov, I., If cell mechanics can be described by elastic modulus: study of different models and probes used in indentation experiments. *Biophys J* **2014,** *107* (3), 564-75.

28. Sokolov, I.; Dokukin, M. E.; Guz, N. V., Method for quantitative measurements of the elastic modulus of biological cells in AFM indentation experiments. *Methods* **2013,** *60* (2), 202-213.

29. Sokolov, I.; Kalaparthi, V.; Kreshchuk, M.; Dokukin, M. E., On averaging force curves over heterogeneous surfaces in atomic force microscopy. *Ultramicroscopy* **2012,** *121*, 16-24.

30. Kuroki, H.; Tokarev, I.; Nykypanchuk, D.; Zhulina, E.; Minko, S., Stimuli-Responsive Materials with Self-Healing Antifouling Surface via 3D Polymer Grafting. *Adv. Funct. Mater.* **2013,** *23* (36), 4593-4600.

31. Fan, Y.; Walish, J. J.; Tang, S. C.; Olsen, B. D.; Thomas, E. L., Defects, Solvent Quality, and Photonic Response in Lamellar Block Copolymer Gels. *Macromolecules* **2014,** *47* (3), 1130-1136.

32. Saito, R.; Kotsubo, H.; Ishizu, K., Synthesis of Microspheres with Hairy Ball Structures from Poly (Styrene-B-2-Vinyl Pyridine) Diblock Copolymers. *Polymer* **1992,** *33* (5), 1073-1077.

33. Chafidz, A.; Ali, I.; Mohsin, M. E. A.; Elleithy, R.; Al-Zahrani, S., Nanoindentation and dynamic mechanical properties of PP/clay nanocomposites. *J Polym Res* **2012,** *19* (7).
34. Schaffer, T. E., Calculation of thermal noise in an atomic force microscope with a finite optical spot size. *Nanotechnology* **2005,** *16* (6), 664-670.
35. Hutter, J. L.; Bechhoefer, J., Calibration of atomic-force microscope tips. *Review of Scientific Instruments* **1993,** *64* (7), 1868-1873.
36. Levy, R.; Maaloum, M., Measuring the spring constant of atomic force microscope cantilevers: thermal fluctuations and other methods. *Nanotechnology* **2002,** *13* (1), 33-37.
37. Sokolov, I.; Zorn, G.; Nichols, J. M., A study of molecular adsorption of a cationic surfactant on complex surfaces with atomic force microscopy. *Analyst* **2016,** *141* (3), 1017-1026.
38. Dokukin, M. E.; Guz, N. V.; Sokolov, I., Quantitative Study of the Elastic Modulus of Loosely Attached Cells in AFM Indentation Experiments. *Biophys J* **2013,** *104* (10), 2123-31.
39. Butt, H. J.; Kappl, M.; Mueller, H.; Raiteri, R.; Meyer, W.; Rühe, J., Steric forces measured with the atomic force microscope at various temperatures. *Langmuir* **1999,** *15*, 2559-2565.
40. Halperin, A.; Zhulina, E. B., Atomic Force Microscopy of Polymer Brushes: Colloidal versus Sharp Tips. *Langmuir* **2010,** *26* (11), 8933-8940.
41. Zdyrko, B.; Klep, V.; Luzinov, I., Synthesis and surface morphology of high-density poly(ethylene glycol) grafted layers. *Langmuir* **2003,** *19* (24), 10179-10187.
42. Dokukin, M. E.; Sokolov, I., Quantitative Mapping of the Elastic Modulus of Soft Materials with HarmoniX and Peak Force QNM AFM Modes. *Langmuir* **2012,** *28* (46), 16060-16071.
43. Dokukin, M. E.; Sokolov, I., On the Measurements of Rigidity Modulus of Soft Materials in Nanoindentation Experiments at Small Depth. *Macromolecules* **2012,** *45* (10), 4277-4288.
44. Grierson, D. S.; Flater, E. E.; Carpick, R. W., Accounting for the JKR-DMT transition in adhesion and friction measurements with atomic force microscopy. *J Adhes Sci Technol* **2005,** *19* (3-5), 291-311.
45. El-Sayed, A.; Masuda, T.; Akita, H.; Harashima, H., Stearylated INF7 peptide enhances endosomal escape and gene expression of PEGylated nanoparticles both in vitro and in vivo. *J Pharm Sci* **2012,** *101* (2), 879-82.

46. Israelachvili, J. N., Intermolecular and Surface Forces Preface to the Third Edition. *Intermolecular and Surface Forces, 3rd Edition* **2011**, Xvii-+.

47. Halperin, A.; Kroger, M.; Zhulina, E. B., Colloid-Brush Interactions: The Effect of Solvent Quality. *Macromolecules* **2011,** *44* (9), 3622-3638.

48. Delcroix, M. F.; Demoustier-Champagne, S.; Dupont-Gillain, C. C., Quartz Crystal Microbalance Study of Ionic Strength and pH-Dependent Polymer Conformation and Protein Adsorption/Desorption on PAA, PEO, and Mixed PEO/PAA Brushes. *Langmuir* **2014,** *30* (1), 268-277.